**Steel and Composite Structures**, *Vol. 35, No. 4 (2020) 475-494*
DOI: https://doi.org/10.12989/scs.2020.35.4.475


# Experimental investigation of shear connector behaviour in composite beams with metal decking

Jawed Qureshi[*1] and Dennis Lam[2a]

*[1]School of Architecture, Computing and Engineering (ACE), University of East London, 4-6 University Way, Beckton, London, E16 2RD, UK*
*[2]School of Engineering, University of Bradford, Bradford, BD7 1DP, UK*

(*Received July 30, 2019, Revised February 28, 2020, Accepted March 5, 2020*)

**Abstract.** Presented are experimental results from 24 full-scale push test specimens to study the behaviour of composite beams with trapezoidal profiled sheeting laid transverse to the beam axis. The tests use a single-sided horizontal push test setup and are divided into two series. First series contained shear loading only and the second had normal load besides shear load. Four parameters are studied: the effect of wire mesh position and number of its layers, placing a reinforcing bar at the bottom flange of the deck, normal load and its position, and shear stud layout. The results indicate that positioning mesh on top of the deck flange or 30 mm from top of the concrete slab does not affect the stud's strength and ductility. Thus, existing industry practice of locating the mesh at a nominal cover from top of the concrete slab and Eurocode 4 requirement of placing mesh 30 mm below the stud's head are both acceptable. Double mesh layer resulted in 17% increase in stud strength for push tests with single stud per rib. Placing a T16 bar at the bottom of the deck rib did not affect shear stud behaviour. The normal load resulted in 40% and 23% increase in stud strength for single and double studs per rib. Use of studs only in the middle three ribs out of five increased the strength by 23% compared to the layout with studs in first four ribs. Eurocode 4 and Johnson and Yuan equations predicted well the stud strength for single stud/rib tests without normal load, with estimations within 10% of the characteristic experimental load. These equations highly under-estimated the stud capacity, by about 40-50%, for tests with normal load. AISC 360-16 generally over-estimated the stud capacity, except for single stud/rib push tests with normal load. Nellinger equations precisely predicted the stud resistance for push tests with normal load, with ratio of experimental over predicted load as 0.99 and coefficient of variation of about 8%. But, Nellinger method over-estimated the stud capacity by about 20% in push tests with single studs without normal load.

**Keywords:** push test; shear stud layout; wire mesh; composite secondary beams; metal decking

## 1. Introduction

Steel-concrete composite construction combines the desirable material properties of steel and concrete. The resulting structural form is efficient, economical and strong. Composite construction has been used since early 1920s. It gained widespread use in bridges in the 1950s and in buildings in the 1960s. Steel-concrete composite beams typically consist of a steel I-section with a floor slab resting on it. The floor slab can be a solid reinforced concrete slab, a pre-cast hollow core slab or a composite slab with profiled sheeting, latter two being more common in modern composite industry.

Steel-concrete composite beam with profiled decking composite slab can be used in primary/secondary beam configurations. Secondary beams support load from the composite slab as a distributed load; and primary beams mainly carry reactions from the secondary beams. Profiled decking is laid parallel to the beam axis in primary beams and perpendicular in secondary beams. This paper is focused on behaviour of composite beams with decking oriented transverse to the longitudinal axis of the beam. Composite action must be ensured when the sheeting is oriented normal to the beam axis. For composite action, shear connectors are generally used. They transfer forces at the steel-concrete interface. Headed studs are the most common form of shear connectors in buildings. The strength of shear connector is normally determined through calibrated push tests in major design codes (David Collings 2013).

Conventional push test setup having a short beam connected to two small concrete slabs (600 × 650 mm in Eurocode 4 (BS EN 1994-1-1 2004) by shear studs has hardly changed ever since its inception in the 1930s. Both concrete slabs remain bedded on the floor and a uniform vertical compressive load is applied to the upper end of the steel beam. This test is used to determine the shear connector strength. Eurocode 4 (BS EN 1994-1-1 2004) recommended push test is for beams with solid slabs; and it does not contain any specific guidance for beams with composite slabs. A general practice has been to use the same solid slab push test arrangement for composite slabs. This has led to lack of ductility in push tests with metal decking, well below the companion beam tests (Qureshi

∗Corresponding author, Ph.D.
E-mail: J.Qureshi@uel.ac.uk
[a] Ph.D.
E-mail: D.Lam1@Bradford.ac.uk


http://www.techno-press.org/?journal=scs&subpage=8
ISSN: 1229-9367 (Print), 1598-6233 (Online)

2010). It is generally believed (Bradford *et al.* 2006, Easterling *et al.* 1993, Hicks 2007, Hicks and Couchman 2004, Hicks and Smith 2014, Smith and Couchman 2010) that the poor ductility is due to absence of a curvature and normal load, which exist in the real beam from the imposed floor loading. Shear stud strength equations for composite beams with metal decking are also primarily based on reduction factors applied to the stud strength with solid slabs. A comprehensive review of these equations is presented elsewhere in Bonilla *et al.* (2018).

Some researchers (Bradford *et al.* 2006, Easterling *et al.* 1993, Nellinger *et al.* 2017, Smith and Couchman 2010) devised the standard push test setup by using a normal load on the top surface of the slab in addition to the shear load. Easterling *et al.* (1993) were the first to use 10% normal load in their standard vertical push test arrangement. Bradford *et al.* (2006) employed a horizontal single-sided push test specimen with a normal load of 5-10% of the shear load, applied along the edges of the specimen to replicate hogging moments in a real beam. The size of specimen was quite large, 1400 × 1200 mm, that enabled a greater number of studs to be placed. They concluded that the conventional vertical push test is not suitable for beams with deep composite slabs. Although, using normal load and horizontal push test setup in Bradford *et al.* (2006) resulted in increase in both stud capacity and slip, the specimens were heavily reinforced. Smith and Couchman (2010) proposed a modification to the standard push test by using a 750 mm × 1000 mm long vertical push test setup with a 12% normal load applied to the faces of the slab. Similarly, using the same test setup, Hicks and Smith (2014) tested four different levels of normal load, 4%, 8%, 12% and 16% of the shear load, and found 12% transverse load to be suitable in terms of the best match with the companion composite beam load-slip behaviour. Both load and slip in (Hicks and Smith 2014, Smith and Couchman 2010) showed considerable enhancement to match with the beam tests. However, increase in the slip could be a result of extra confinement effect produced by the spreader beams used to apply normal load. Fixing these beams to the test slab could also have delayed onslaught of slip at the steel-concrete interface.

Qureshi *et al.* (2011) conducted preliminary push tests, using the same test setup as this paper, just to validate their numerical model. This seminal research predicted the post-failure behaviour of the push test through numerical modelling for the first time. Nellinger *et al.* (2014, 2017, 2018) studied the effect of concentric and eccentric normal load on slip and stud strength. They used 8% and 16% of the shear load as the normal load and recommended a concentric normal load of 10% of the shear load for push tests with stud to deck height ratio equal to or less than 1.56. For tests with stud-to-deck height ratio more than 1.56, transverse (normal) load was not needed. However, eccentric normal loading, used to represent negative moments in slabs, did not have much influence on load-slip behaviour of the stud. In the USA, Rambo-Roddenberry (2002) carried out comprehensive push tests with 5-20% normal loads and proposed an empirical stud strength prediction model, mainly using American deck profiles. Current AISC 360-16 (ANSI/AISC 360-16 2016) provisions for strength of headed shear stud anchors are based on Rambo-Roddenberry's (Rambo-Roddenberry 2002) empirical design equations.

Other developments in last two decades include use of stud performance enhancing reinforcement to inhibit rib shear failure in edge beams. Use of this innovative reinforcement originated in Australia. Patrick (2000) was the first to use waveform reinforcement components to prevent rib shearing failure in composite edge beams. Ernst *et al.* (2009, 2010) used the waveform reinforcement and stud performance enhancing devices to address the problem of low ductility of the stud. Shen and Chung (2017a and 2017b) studied the behaviour of solid and composite slabs under shear forces and combined shear and tension forces. They found that presence of tension forces reduced the stud resistance by 75% in push tests with composite slabs. Monotonic and cyclic behaviour of studs in composite slabs was investigated by Sun *et al.* (2019). Three test parameters were studied: deck type, deck orientation and loading conditions. The authors argued that through-welded studs had weld flaws, which could be alleviated by additional welding. Huo *et al.* (2019) conducted static and dynamic push tests to study the stud behaviour in composite beams. They proposed a prediction method for dynamic shear capacity of a stud placed in a deck oriented parallel to the beam.

Although the slip at steel-concrete interface in earlier studies (Bradford *et al.* 2006, Ernst *et al.* 2009, Hicks and Smith 2014, Nellinger *et al.* 2014, 2017, Patrick 2000, Smith and Couchman 2010) met the Eurocode 4 (BS EN 1994-1-1 2004) requirement of 6 mm slip for ductile stud failure, the push test specimens were either heavily reinforced or overly confined. Our study uses a single-sided horizontal push test arrangement with a 1500 × 1500 mm composite slab, more than double the size of the standard vertical push test (600 × 650 mm). This setup has four main advantages: first – longer slabs allow greater distribution of shear forces by having more studs, second – wider slabs help prevent premature rib shear failure that happens in the conventional vertical push test due to limited width of the deck profile, third – single-sided slab allows symmetrical transfer of shear load and fourth – consistent concrete strength is maintained in the slab as only one slab needs to be cast. The longer slab enables five stud rows to be placed representing more closely full-scale composite beams. Some push tests use normal load besides shear loading. Additional confinement from normal load is prevented by using a roller base fixture under the normal loading point. This allows smooth movement of the specimen under shear load while keeping the normal load constant.

The position of wire mesh within a steel deck can affect the stud's behaviour. General practice within composite decking industry is to use the mesh at a nominal cover from top of the concrete slab for crack control and longitudinal shear (Smith and Couchman 2010). However, Eurocode 4 (BS EN 1994-1-1 2004) suggests using a mesh at 30 mm below the stud head. This position can roughly be on top of the deck in some cases; but may not be practically possible in many composite steel decks. Limited research (Nellinger

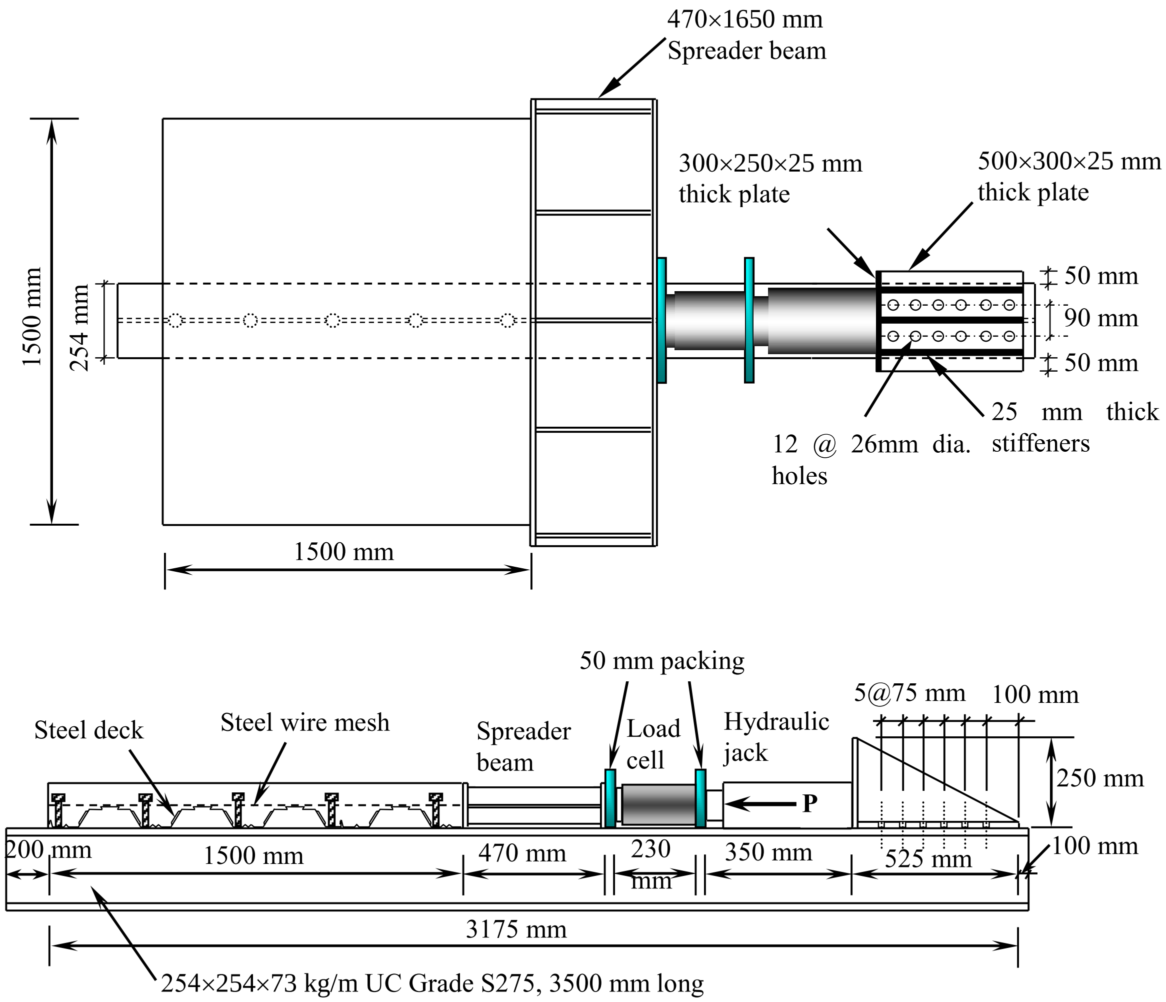


Fig. 1 Single-sided horizontal push test arrangement used for testing

*et al.* 2017, Smith and Couchman 2010) exists on influence of mesh position and number of layers on shear stud behaviour. More research is needed to see if laying a mesh layer on top of steel deck or at a nominal cover from top surface of the concrete slab or combination of both has any effect. Use of a bar reinforcement near the bottom trough is recommended by some decking manufacturers (Kingspan 2011) for composite action and fire performance. No independent research is available to verify effectiveness of this bar. Further experimental research is required to validate the usefulness of the reinforcing bar in ensuring composite action.

Tests are conducted on 24 full-scale push test specimens to study the behaviour of headed shear studs in steel-concrete composite beams with profiled decking laid normal to the beam axis. Four main variables are investigated to see if the design standard provisions and current practice within composite decking are appropriate. These include, effect of wire mesh position and number of its layers, using a reinforcing bar in the bottom trough of the deck rib, normal load and its position, and shear stud layout. The test results are discussed in terms of strength, ductility and failure modes. A comparison of test results is also presented with design equations from Eurocode 4 (BS EN 1994-1-1 2004), Johnson and Yuan (Johnson and Yuan 1998), AISC 360-16 (ANSI/AISC 360-16 2016) and Nellinger *et al.* (Nellinger *et al.* 2018).

## 2. Experimental Investigation

Push tests are used to study the shear connector behaviour in composite beams. The experimental investigation is divided into two series. The first series contains only shear loading; while the second has a normal load additional to the shear load. The normal load is assumed to be 10% of the applied shear load. The steel beam in real life supports longer spans of composite slabs than the lab push test slabs. This is replicated by applying a normal load to the composite slab in the push test. A normal load roughly equal to 10% of the horizontal shear load is considered equivalent to the self-weight of the composite slab in a real-life situation.

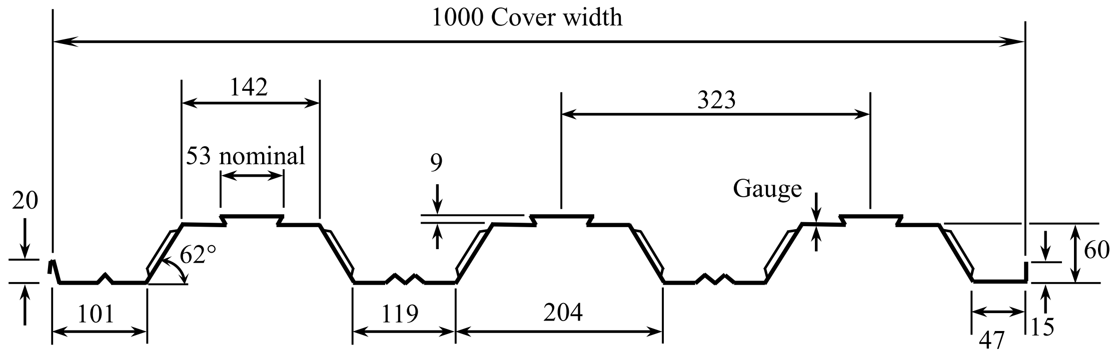


Fig. 2 Geometry and dimensions of 60 mm deep trapezoidal deck profile

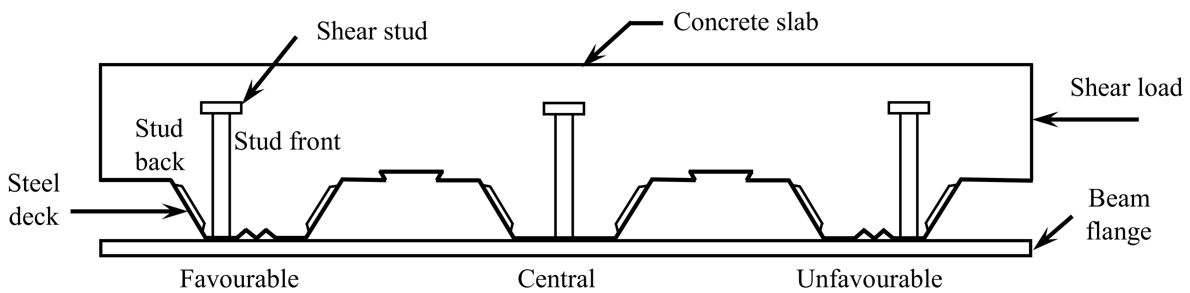


Fig. 3 Shear studs in favourable (strong), central and unfavourable (weak) positions in a push test

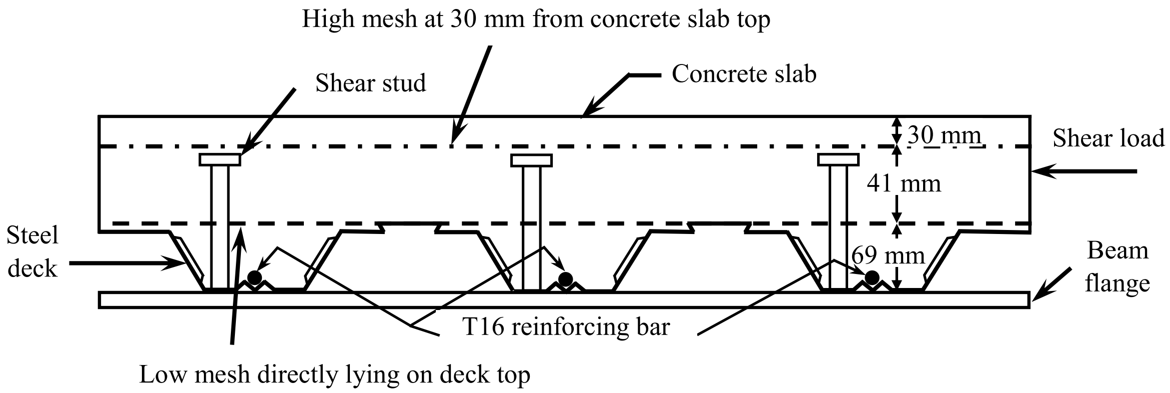


Fig. 4 Details of mesh position and T16 reinforcing bar

### *2.1 Test arrangement and instrumentation*

Fig. 1 shows a single-sided horizontal push test arrangement used for all push tests. The composite slab is 1500×1500 mm and 140 mm deep. Fig. 2 represents a Multideck 60-V2 profiled sheeting from Kingspan (Kingspan 2011). The sheeting is 60 mm deep ($h_p$), 150 mm wide ($b_o$) and 0.9 mm thick ($t$). Headed shear studs 19 mm × 100 mm are welded through the sheeting to the 3500 mm long 254 × 254 × 73 UC steel beam. The studs are welded to the favourable side of the deck profile. A favourable or strong position is when the volume of concrete in front of the stud, in the direction of applied shear load, is greater than the volume behind it. In a simply supported beam, studs placed at the side away from the point of maximum bending moment (midspan) are favourably located studs (Qureshi *et al.* 2011). Studs welded to favourable, central and unfavourable positions are shown in Fig. 3. Majority of modern steel decking have a central stiffening rib, resulting in a favourable (strong) or unfavourable (weak) stud position. For tests with double studs per rib, a centre-to-centre transverse spacing of 100 mm is maintained in all five ribs.

A standard square welded wire mesh fabric A193 is laid on the sheeting. This mesh has 7 mm diameter bars with 200 mm centre to centre spacing both ways. Three different mesh positions were used – high, low and double. High position had a mesh placed at 30 mm from top surface of

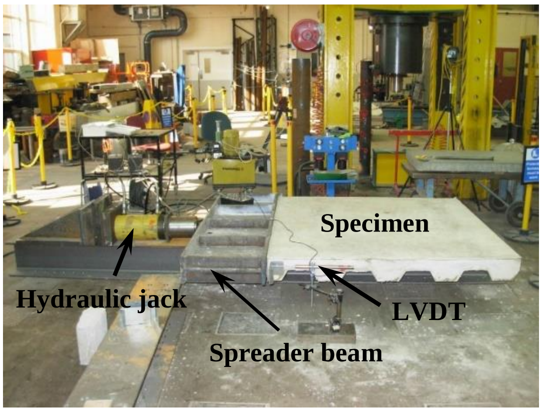


(a) First series

(b) Second series with normal load

Fig. 5 General test arrangement for push test

the concrete slab, while low position had the mesh rested directing on top flange of the sheeting and double position had a combination of both high and low mesh layers. Fig. 4 shows the exact location of low and high mesh, and T16 reinforcing bar. All specimens were cast horizontally as suggested in Eurocode 4 (BS EN 1994-1-1 2004). Cubes and cylinders for compressive and tensile strength tests were also cast simultaneously.

The test rig consisted of a 100-tonne hydraulic jack, with a stroke of 250 mm, placed at the centre of the specimen. The horizontal load was applied at the centre of the spreader beam with the help of a hydraulic jack and measured through a load cell. Fig. 5 shows complete push test set up with Fig. 5(a) showing the first series and Fig. 5(b) representing the second series with normal load. The pressure was supplied to the hydraulic jack with the help of Enerpec hydraulic pump. The relative slip between the slab and the steel deck is measured by two linear voltage displacement transducers (LVDTs), mounted on the sides of concrete slab adjacent to the spreader beam.

The test set up for second series, Fig. 5(b), was essentially the same as the first one, except normal load application. The normal load was applied with the help of two spreader beams placed on the top surface of the concrete slab. A steel plate was placed on the spreader beams to distribute the load equally. The hydraulic jack and load cell were positioned at the centre of this steel plate. To allow horizontal movement of the push test specimen, a roller track was located beneath the load cell. Except one LVDT placed on top of the concrete slab to measure its uplift, all other instrumentation remained the same as the first series.

### 2.2 Loading procedure

Each test contained a minimum of two specimens. First specimen had load applied in 40 kN increments up to 60% of the expected failure load and reduced to 10 kN increments afterwards. The expected failure load was established from Eurocode 4 (BS EN 1994-1-1 2004) provisions. The failure load obtained from the first specimen was used as a reference failure load for the second specimen. The second specimen was loaded up to 40% of the failure load and cycled 25 times between 5% and 40% of the failure load as per Eurocode 4 Annex B.2.4 (BS EN 1994-1-1 2004). Thereafter, load increments were reduced in such a way, so that failure did not occur in less than 15 minutes. The purpose of cyclic loading was to break any chemical bond between profiled sheeting and concrete slab. Chemical bond is formed due to chemical adherence of cement paste to the steel sheeting. The longitudinal slip between concrete slab and steel beam was continuously measured until the load dropped to at least 20% below the maximum failure load.

For second series, a normal load of 10% of the maximum horizontal shear load was applied to the specimen, before applying the horizontal shear load. The maximum horizontal shear load was established from the companion push tests conducted earlier without normal load. The normal load remained constant during the entire test. The horizontal shear load was applied, while keeping the normal load constant, until the concrete slab completely separated from the steel deck.

### 2.3 Material testing

The material properties of concrete, reinforcing bars, shear connector and steel deck were obtained from various material tests. The compressive strength of concrete was determined by testing three cylinders (150×300 mm) and cubes (100×100×100 mm) on the day of the test. The growth of concrete strength was monitored by testing two cubes at each 7 and 14 and 28 days. Concrete compressive strengths are presented in Table 1. The tensile test on T16 high yield reinforcing bar was conducted using the Instron universal testing machine according to BS EN ISO 6892-1:2009 (BS EN ISO 6892-1 2009). The yield and ultimate strengths were obtained from the tensile test. The same machine was used to test tensile coupons machined from Nelson shear studs. The modulus of elasticity, yield stress and ultimate strength for the shear stud material were found to be 193 GPa, 563 MPa and 611 MPa, respectively. Tensile coupons were also machined from the steel deck profile to determine its material properties. The mean values for the elastic modulus, yield stress and ultimate tensile strength

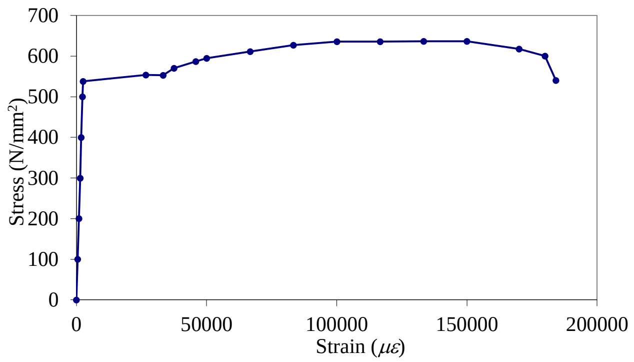


(a) T16 reinforcing bar

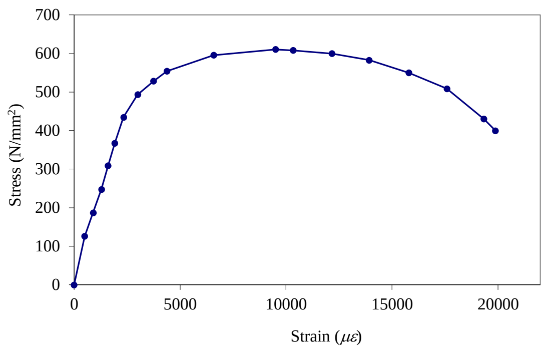


(b) Shear stud

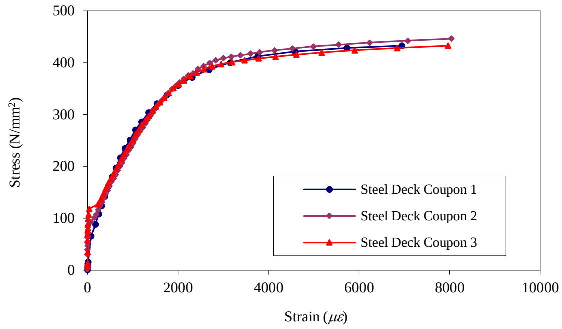


(c) Steel deck

Fig. 6 Stress-strain curve for steel components

were 210 GPa, 418 MPa and 437 MPa, respectively. The stress-strain curves for T16 bar, shear stud and steel deck are all presented in Fig. 6.

## 3. Results and discussion

Table 1 presents test parameters and summary of push test results. Each test had two nominally identical specimens for statistical acceptance of the test results. Specimen labels are given in column 3, which identify number of studs per rib, presence of normal load and mesh layers. The letters P or PT denote push test, S and D indicate single and double stud per rib, N specifies the normal load and M is for double mesh. First series had only shear loading; while second had a combination of shear and normal load. In first series, the test PTS 1 and 2 had a single stud per rib with low and high mesh position, respectively. While PTD 1 and 2 had double studs with high mesh and a T16 bar placed between two central pultruding ribs at the bottom trough in the latter test as shown in Fig. 4. In second series, PTSN 1 and 2 had same test parameters as PTS 1 and 2, except a 10% normal load was applied parallel to the steel beam axis. PTDN 1 and 2 had double studs and high mesh. There were no studs in the last rib of PTDN 2. Also, PSNM 1 and 2 had no stud in the last rib. Both tests contained single stud per rib with double mesh layer. In PSNM 2, the position of normal load was directly on top of the first rib perpendicular to the beam axis in contrast to PSNM 1, where normal load was applied parallel to the beam axis. The test PDNM 1 had no studs in the last rib; and PDNM 2 contained studs in middle three ribs only – first and last ribs were unstudded. They had double studs and two mesh layers; and the normal load position was same as PSNM 1 – parallel to the beam axis.

Concrete strength affects the shear connector resistance. For realistic comparison of different parameters, concrete strength must be same for all specimens. However, it is not practically possible to test all specimens on the same day, and thus, ensure same concrete strength. An alternative approach is to normalise the stud strength of all tests to a common concrete strength. Therefore, the experimental shear connector resistances, $P_e$, have been normalised to a common concrete cube strength of 30 N/mm$^2$ in proportion to the square root of cube strength, $f_{cm,cube}$ of the push test using Equation (1). This equation has previously been used by Lloyd and Wright (1990). The normalised strength, $P_{e,norm}$ is presented in Table 2.

$$P_{e,norm} = \frac{P_e}{\sqrt{\dfrac{f_{cm,cube}}{30}}} \tag{1}$$

### *3.1 Effect of mesh position and number of mesh layers*

The effect of mesh position was studied in push tests PTS 1 and 2, and PTSN 1 and 2 when normal load was present. Both tests, PTS 1 and 2, had a single stud per rib

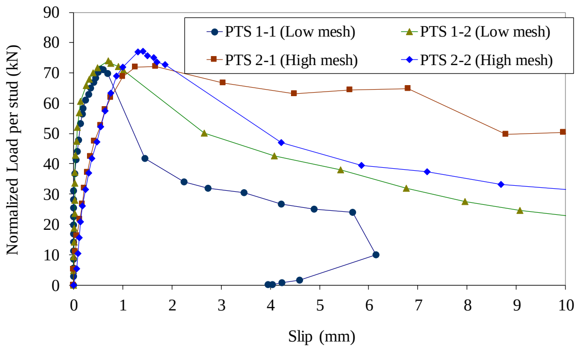


Fig. 7 Effect of mesh position

Table 1 Test parameters and summary of push test results

| Series | S. No. | Test Ref. | Concrete cube strength (MPa) | No. of Studs per rib, $n_r$ | Total No. of studs per specimen | Studs in first rib | Studs in last rib | Mesh position | No. of mesh layers | Extra bar | Normal load | Shear capacity per stud (kN) |
|---|---|---|---|---|---|---|---|---|---|---|---|---|
| (1) | (2) | (3) | (4) | (5) | (6) | (7) | (8) | (9) | (10) | (11) | (12) | (13) |
| First | 1 | PTS 1-1 | 34.0 | 1 | 5 | Yes | Yes | Low | Single | --- | --- | 75.7 |
| | 2 | PTS 1-2 | 34.0 | 1 | 5 | Yes | Yes | Low | Single | --- | --- | 78.8 |
| | 3 | PTS 2-1 | 27.5 | 1 | 5 | Yes | Yes | High | Single | --- | --- | 69.0 |
| | 4 | PTS 2-2 | 27.5 | 1 | 5 | Yes | Yes | High | Single | --- | --- | 73.8 |
| | 5 | PTD 1-1 | 27.9 | 2 | 10 | Yes | Yes | High | Single | --- | --- | 52.1 |
| | 6 | PTD 1-2 | 27.9 | 2 | 10 | Yes | Yes | High | Single | --- | --- | 45.4 |
| | 7 | PTD 2-1 | 28.0 | 2 | 10 | Yes | Yes | High | Single | T16 | --- | 52.2 |
| | 8 | PTD 2-2 | 28.0 | 2 | 10 | Yes | Yes | High | Single | T16 | --- | 47.3 |
| Second | 9 | PTSN 1-1 | 25.4 | 1 | 5 | Yes | Yes | Low | Single | --- | 10% | 97.8 |
| | 10 | PTSN 1-2 | 25.4 | 1 | 5 | Yes | Yes | Low | Single | --- | 10% | 98.9 |
| | 11 | PTSN 2-1 | 21.2 | 1 | 5 | Yes | Yes | High | Single | --- | 10% | 90.0 |
| | 12 | PTSN 2-2 | 23.2 | 1 | 5 | Yes | Yes | High | Single | --- | 10% | 81.7 |
| | 13 | PTDN 1-1 | 28.2 | 2 | 10 | Yes | Yes | High | Single | --- | 10% | 61.3 |
| | 14 | PTDN 1-2 | 37.0 | 2 | 10 | Yes | Yes | High | Single | --- | 10% | 67.3 |
| | 15 | PTDN 2-1 | 58.8 | 2 | 8 | Yes | No | High | Single | --- | 10% | 91.3 |
| | 16 | PTDN 2-2 | 63.2 | 2 | 8 | Yes | No | High | Single | --- | 10% | 93.7 |
| Second | 17 | PSNM 1-1 | 32.8 | 1 | 4 | Yes | No | Low & High | Double | --- | 10% | 113.0 |
| | 18 | PSNM 1-2 | 36.1 | 1 | 4 | Yes | No | Low & High | Double | --- | 10% | 138.4 |
| | 19 | PSNM 2-1 | 32.3 | 1 | 4 | Yes | No | Low & High | Double | --- | 10% | 127.2 |
| | 20 | PSNM 2-2 | 32.7 | 1 | 4 | Yes | No | Low & High | Double | --- | 10% | 134.6 |
| | 21 | PDNM 1-1 | 46.0 | 2 | 8 | Yes | No | Low & High | Double | --- | 10% | 72.7 |
| | 22 | PDNM 1-2 | 48.8 | 2 | 8 | Yes | No | Low & High | Double | --- | 10% | 81.8 |
| | 23 | PDNM 2-1 | 30.7 | 2 | 6 | No | No | Low & High | Double | --- | 10% | 77.3 |
| | 24 | PDNM 2-2 | 31.6 | 2 | 6 | No | No | Low & High | Double | --- | 10% | 76.8 |

Note: Mesh located at low position is resting on top of the steel deck and high location is 30 mm below the top surface of the concrete slab. T16 bar is placed at the centre of the bottom flange of the sheeting. Normal load is applied as 10% of the horizontal shear load parallel to the beam axis except PSNM 2, where it is applied on top of the first rib normal to beam axis

and the mesh located at low and high position, respectively. Fig. 7 shows the normalised load versus slip curves for these push tests. The mean strength for PTS 1 is 72.6 kN and for PTS 2 it is 74.6 kN as shown in Table 2. This suggests only a marginal change in the stud's strength. The discrepancy in the initial stiffness of the load-slip behaviour between PTS 1 and PTS 2 is due to different position of displacement transducer, placed at the back of the slab in PTS 1 and at the loaded side of the slab in PTS 2.

Fig. 7 shows that post-peak ductility for tests with high mesh is slightly higher than low mesh tests. Until now it is commonly believed that a low mesh can possibly increase ductility and delay concrete pull-out failure. However, our results suggest otherwise. In real terms, the marginal increase in post-peak ductility with high mesh may not improve overall ductility of the composite beams. Looking at Fig. 4, it is evident that both low and high mesh do not interfere with concrete failure cones, which start from the stud's head progressing down to the deck's top flange. This means, in principle, a single layer of mesh either low or high cannot prevent concrete failure. This can be different though in double mesh layer, where an extra mesh layer could confine concrete and increase the strength or ductility of stud.

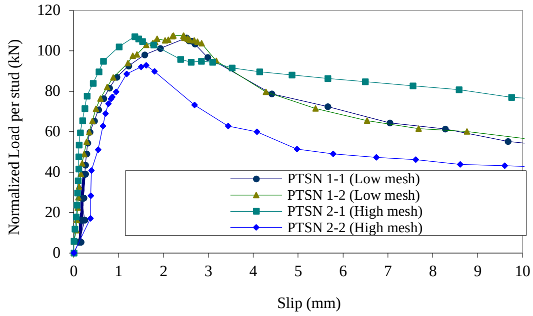


Fig. 8 Effect of mesh position for tests with horizontal shear and normal load

The same test configuration is repeated in PTSN 1 and 2 with 10% normal load. The average normalised strength for PTSN 1 is 107 kN with COV of 0.8% and it is 100 kN for PTSN 2 with COV of 10.1% as shown in Table 2. The normalised load versus slip curves for single stud push tests with normal load are plotted in Fig. 8. Again, the results indicate that mesh location has no influence on the shear connector resistance and slip. Thus, within the limits tested in this research, it is concluded that locating the mesh either directly in low or high position does not affect the strength and ductility of the headed shear stud. This is different to the findings in Smith and Couchman (2010), where positioning the mesh on top of the deck (low mesh) showed 31% improvement in stud capacity. This increase in stud strength could be due to the extra confinement provided by spreader beams used to apply normal load in Smith and Couchman (2010). These beams were fixed to the loading frame, which could have enhanced the confinement effect. Contrarily, this study uses a roller track on top of the normal load spreader beam underneath the hydraulic jack. This set up ensures that normal load applied does not result in unintended additional confinement effect.

Typical failure mode was concrete cone failure, where cracking started from under the stud's head and progressed to top of the steel deck. Placing the mesh on top of the deck may not cross the failure surfaces of concrete cone perpendicularly. That is the reason for no improvement in stud capacity when mesh is located below the head of shear stud. Strength enhancement could have been achieved if either waveform or spiral reinforcement, similar to Ernst *et al.* (2009, 2010) and Patrick (2000), was used around the stud or mesh was placed normal to concrete failure surfaces. However, in practice, placing reinforcement normal to the failure lines may not be practical.

The effect of single and double mesh layer is investigated in push tests PTSN and PSNM for single stud per rib, and PTDN and PDNM for double studs per rib. Table 2 shows that the mean normalised load per stud for PTSN 1 and 2 is 107 kN and 100 kN. Corresponding mean load in PSNM 1 and 2 with double mesh layer is 117.2 kN and 125.8 kN. This suggests an increase of 17% on average when double mesh layer is used in tests with single studs per rib. For tests with double studs, mean normalised load per stud for PTDN 1 having high mesh is 61.9 kN compared with 61.4 kN in PDNM 1 with double mesh. Both tests had normal load and no studs in the last rib. This clearly shows that having double mesh layer does not improve shear stud strength in tests with double studs per rib.

In contrast, Nellinger *et al.* (2017) reported a 47% increase in stud strength with use of a double mesh layer compared with the single layer. They used 80 mm deep deck, 160 mm deep slab, centrally placed double studs (19.1 × 118.2 mm), and 0.9 mm thick and 137.5 mm wide ($b_o$) deck. In their study (Nellinger *et al.* 2017), single and double studs per rib showed no difference in failure load per stud. It is generally believed that load per stud in tests with double studs per rib is 30% lower than single stud per rib due to concrete failure cones around studs sharing failure planes in stud pairs. This large increase in the stud resistance, by using a double mesh layer in Nellinger *et al.* (2017), could be due to different deck geometry, mesh size and layout. Our study used A193 mesh – 7 mm diameter bar at 200 mm centre-to-centre spacing and low mesh rested on top of the steel deck and high mesh was 30 mm below the slab's top surface. This gave 50 mm spacing between two mesh layers.

The low mesh in Nellinger *et al.* (2017) consisted of Q118A mesh – 6 mm dia at 150 mm c/c placed 15 mm above the steel deck flange and the high mesh, Q335A – 8 mm dia at 150 mm c/c, was located at 31 mm from the slab's top. This resulted in 34 mm spacing between two layers along the slab's depth. On the other hand, their control specimen (Nellinger *et al.* 2017), with a single mesh layer (Q118A), had the mesh positioned at 30 mm above the deck. Perhaps, the large diameter of high mesh and low centre-to-centre spacing of mesh could be the reason for 47% increase in the stud strength with a double mesh layer in Nellinger *et al.* (2017).

Main failure mode in tests PTS 1 and 2, with low and high mesh, was concrete related. The load application was continued until the concrete slab completely detached from the profiled metal decking and shear studs. At failure, a deep crack appeared in the last studded rib of the specimen near the top flange of the steel deck. It continued to widen resulting in rotation of the last rib. Both tests failed by a combination of concrete conical failure and rotation of the last studded rib, typically known as 'back-breaking' failure as shown in Fig. 9 (a) and 9(b). In case of concrete cone failure, the tensile force acting on the stud forces the concrete slab to move up and ride over the metal decking,

(a) Rotation of last rib/back-breaking failure in PTS 1-1

(b) Concrete failure cones in PTS 1-1

(c) Stud pullout and concrete cones in PTS 1-2

(d) Underside of slab in PTS 1-2 showing concrete pull-out failure surfaces

Fig. 9 Comparison of failure modes in tests with low and high mesh

and consequently leaving behind a concrete failure cone around the shear stud.

The size of these failure cones in middle three ribs was about 50% larger than the first and last rib. The first stud in the push test PTS 1-2 sheared off, and the last stud completely detached from the steel deck and remained embedded inside the concrete rib as shown in Fig. 9(c). The underside of the concrete slab in the specimen PTS 1-2 showing concrete pull-out failure surfaces is presented in Fig. 9(d). Shearing of first stud and pulling of last stud indicates a non-uniform response of studs along the longitudinal direction. The last stud is pulled due to rotation of the rib and the first stud is sheared due to proximity to load application point. This suggests that the distribution of shear load along longitudinal direction is not uniform. The first and last stud could not utilise their full capacity.

Tests with double studs failed in a similar fashion. Due to 100 mm spacing between two studs, concrete failure cones did not form separately and coincided with each other creating a wedge shape. Tests with normal load using both single and double studs had the same failures modes as the tests without normal load. Mesh layers and number did not affect failure patterns either.

### *3.2 Effect of reinforcement bar in deck rib*

The effect of an extra T16 reinforcement bar placed at the bottom of the trough is investigated in push tests PTD 1 and PTD 2 with double studs per rib. The push test PTD 2 had an extra T16 high yield reinforcement bar at the bottom of the sheeting pan and PTD 1 was without it. The mean normalised shear connector resistance for PTD 1 is 50.6 kN with COV of 9.8% and PTD 2 is 51.5 kN with COV 0f 7% as shown in Table 2. The normalised load per stud versus slip curves are plotted in Fig. 10. Table 2 shows that the average shear connector resistance obtained from the push test with reinforcement bar is not much different from the one without it. Some manufacturers, like Kingspan (2011), recommend using a 16 mm diameter reinforcement bar in every trough of their 146 mm deep profiled sheeting for composite action and fire design performance. One key finding from this study is that suspending a bar at bottom of the trough neither affects strength nor ductility of the headed stud. Thus, using a reinforcement bar at the bottom of the trough is redundant and does not contribute to composite beam action.

After failure, concrete wedges were formed around the pair of shear connectors. For push tests with double shear studs per rib (PTD1 and PTD2), failure lines initiated from the underside of the stud and progressed to the bottom flange of the deck. The individual concrete failure cones formed in this way remained connected between two studs creating a concrete failure wedge, as shown in Fig 11(a) for PTD 1-2. All shear studs remained attached to the steel beam after failure. The first and last two studs bent in the direction of the loading, while studs in the middle three troughs remained unchanged. The development of concrete failure wedges was also approximately same in all double studs push tests except in the push test PTD 2, where some concrete fragments remained attached to the reinforcement bar as seen in Fig. 11(b). However, these concrete broken

Table 2 Determination of normalised shear connector resistance

| | S No. | Test Ref. | No. of Studs $n_r$ | $f_{cm,cube}$ (MPa) | $P_e$ (kN) | $P_{e,norm}$ (kN) | Mean ($P_{e,norm}$) | SD ($P_{e,norm}$) | COV ($P_{e,norm}$) |
|---|---|---|---|---|---|---|---|---|---|
| (1) | (2) | (3) | (4) | (5) | (6) | (7) | (8) | (9) | (10) |
| First | 1 | PTS 1-1 | 1 | 34.0 | 75.7 | 71.1 | 72.6 | 2.1 | 2.8% |
| | 2 | PTS 1-2 | 1 | 34.0 | 78.8 | 74.0 | | | |
| | 3 | PTS 2-1 | 1 | 27.5 | 69.0 | 72.1 | 74.6 | 3.5 | 4.7% |
| | 4 | PTS 2-2 | 1 | 27.5 | 73.8 | 77.1 | | | |
| | 5 | PTD 1-1 | 2 | 27.9 | 52.1 | 54.1 | 50.6 | 4.9 | 9.8% |
| | 6 | PTD 1-2 | 2 | 27.9 | 45.4 | 47.1 | | | |
| | 7 | PTD 2-1 | 2 | 28.0 | 52.2 | 54.0 | 51.5 | 3.6 | 7.0% |
| | 8 | PTD 2-2 | 2 | 28.0 | 47.3 | 48.9 | | | |
| Second | 9 | PTSN 1-1 | 1 | 25.4 | 97.8 | 106.4 | 107.0 | 0.8 | 0.8% |
| | 10 | PTSN 1-2 | 1 | 25.4 | 98.9 | 107.6 | | | |
| | 11 | PTSN 2-1 | 1 | 21.2 | 90 | 107.1 | 100.0 | 10.1 | 10.1% |
| | 12 | PTSN 2-2 | 1 | 23.2 | 81.7 | 92.8 | | | |
| | 13 | PTDN 1-1 | 2 | 28.2 | 61.3 | 63.2 | 61.9 | 1.8 | 3.0% |
| | 14 | PTDN 1-2 | 2 | 37.0 | 67.3 | 60.6 | | | |
| | 15 | PTDN 2-1 | 2 | 58.8 | 91.3 | 65.2 | 64.9 | 0.4 | 0.7% |
| | 16 | PTDN 2-2 | 2 | 63.2 | 93.7 | 64.6 | | | |
| Second | 17 | PSNM 1-1 | 1 | 32.8 | 113.0 | 108.1 | 117.2 | 12.8 | 10.9% |
| | 18 | PSNM 1-2 | 1 | 36.1 | 138.4 | 126.2 | | | |
| | 19 | PSNM 2-1 | 1 | 32.3 | 127.2 | 122.6 | 125.8 | 4.5 | 3.5% |
| | 20 | PSNM 2-2 | 1 | 32.7 | 134.6 | 128.9 | | | |
| | 21 | PDNM 1-1 | 2 | 46.0 | 72.7 | 58.7 | 61.4 | 3.8 | 6.2% |
| | 22 | PDNM 1-2 | 2 | 48.8 | 81.8 | 64.1 | | | |
| | 23 | PDNM 2-1 | 2 | 30.7 | 77.3 | 76.4 | 75.6 | 1.1 | 1.5% |

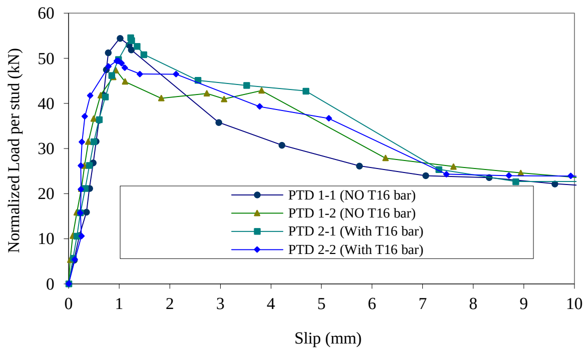


Fig. 10 Normalised load versus slip curves for double studs push tests with horizontal shear loading only

bits near the reinforcement bar at the bottom trough did not contribute towards increase in either strength or ductility. Use of T16 bar did not increase the size of concrete wedges either. The additional bar could have increased the shear connector strength, and possibly the ductility, if it was placed at a location closer to concrete failure surfaces.

### *3.3 Effect of normal load and its position*

The normalised load per stud versus slip curves for single and double stud push tests with and without 10% normal load are plotted in Figs. 12 and 13, respectively. The tests PTS and PTD are without normal load and PTSN and PTDN are with 10% normal load. The strength enhancement of about 40% and 23% was achieved in single and double studs per rib by applying normal. This increase is due to confinement of concrete around shear connectors because of normal load.

The strength enhancement in the single stud per rib tests was twice as compared with double studs per rib. The stud strength depends on how large concrete failure cones are around the stud. In double studs the failure cones are shared between two studs and cannot develop fully. In contrast, in single stud per rib these cones form individually around the stud. This is the reason for almost half increase in strength for double studs compared with single studs per rib. Despite significant increase in the shear connector resistance, the ductility of the shear connector could not be improved. The effect of normal load position is studied in push tests PSNM 1 and PSNM 2. The test PSNM 1 had normal load applied to the centre of the concrete slab parallel to the beam axis as shown in Fig. 14(a). For PSNM 2, the normal load position was just above the first rib of the sheeting perpendicular to the beam axis as seen in Fig. 14(b). Tests shown in Fig 13 had no difference in failure patterns, with both tests failing due to concrete cone formation. The normalised load per stud versus slip curves for both push tests PSNM 1 and PSNM 2 are presented in Fig. 15. The average shear connector resistance obtained from push tests PSNM 1 and PSNM 2 was 117.2 kN and 125.7 kN, respectively. Due to very small difference in load per stud in these tests, it is fair to conclude that normal load position has no effect on the stud strength.

(a) Concrete failures wedges for push test PTD 1-2 (without T16 bar)

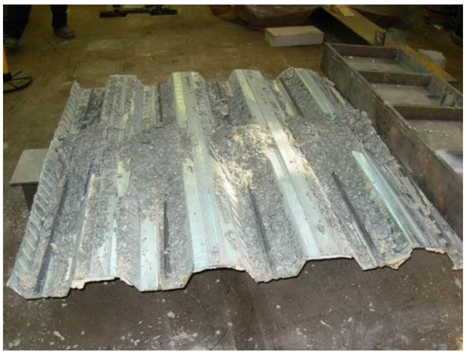

(b) Concrete failure cones in PTD 2-1 (with T16 bar)

Fig. 11 Comparison of failure modes in tests with or without T16 bar

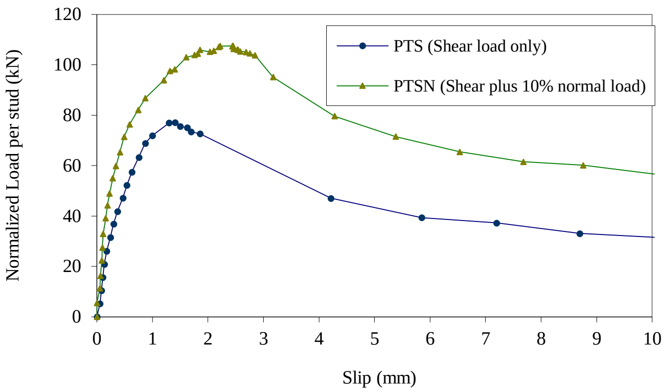


Fig. 12 Comparison of push tests having single stud per rib with and without normal load

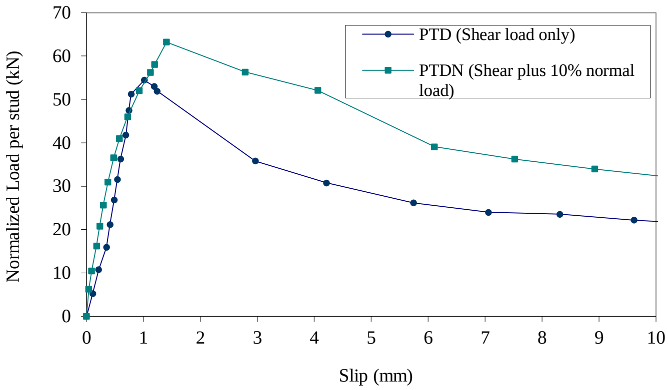


Fig. 13 Comparison of push tests having double studs per rib with and without normal load

(a) Specimen PSNM 1-2 after failure with normal load parallel to beam axis

(b) Specimen PSNM 2-1 after failure with normal load on first rib perpendicular to beam axis.

Fig. 14 Comparison of position of normal load

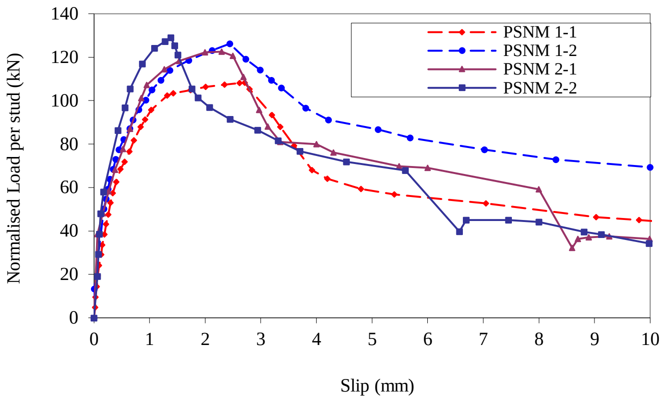


Fig. 15 Effect of normal load position

### *3.4 Effect of shear stud arrangement*

Stud arrangement within a push test affects failure mechanisms. For example, when all five ribs are studded, the last rib rotates, and back-breaking failure happens. The main question here is whether it influences the shear connector capacity or not. Three configurations are tried with studs in all five ribs, first four ribs and middle three ribs. PTDN 1 and 2 present the first comparison with studs in all ribs and first four ribs. Table 2 shows the average normalised shear connector resistance as 61.9 kN and 64.9 kN for PTDN 1 and 2 with coefficient of variation of 3% and 0.7%, respectively. Fig. 16 presents the normalised load per stud versus slip curves for both tests. Keeping the last rib unstudded prevented its rotation and helped avoid unwanted back-breaking failure. However, it did not affect the strength and ductility of the stud as seen in Fig. 16.

The second comparison includes PDNM 1 and 2 with studs in first four and middle three ribs, respectively. The normalised load per stud for PDNM 1 and 2 is 61.4 kN and 75.6 kN, respectively. The load-slip curves for both tests are presented in Fig. 17. Both tests had double mesh layers and normal load applied. The strength in tests with studs in middle three ribs was 23% higher than the stud strength in push test with last rib unstudded (studs in first four ribs). The reason for this increase is due to shear force distribution in the longitudinal direction of the slab. Removing studs from the first and last rib allows shear load on middle three studs to be distributed more evenly, resulting in higher load per stud as large concrete volume is available in front of the first stud. For push tests with studs in first four ribs, shear stud in first rib shears off quickly resulting in a lower load per stud due to limited concrete volume in front of stud. However, the ductility of the shear stud remained unaffected by the stud's arrangement within a rib.

## 4. Comparison with stud strength prediction methods

The push test results are compared to the predicted strengths from Eurocode 4 (BS EN 1994-1-1 2004) equations, Johnson and Yuan (Johnson and Yuan 1998) method, AISC 360-16 (ANSI/AISC 360-16 2016) provisions and Nellinger *et al.* (2018) equations. The experimental shear connector strengths are plotted against predicted strengths to see how well the existing strength prediction methods estimate the shear connector resistance. Predicted shear stud connector strengths from these methods are characteristic values without using any partial safety factors.

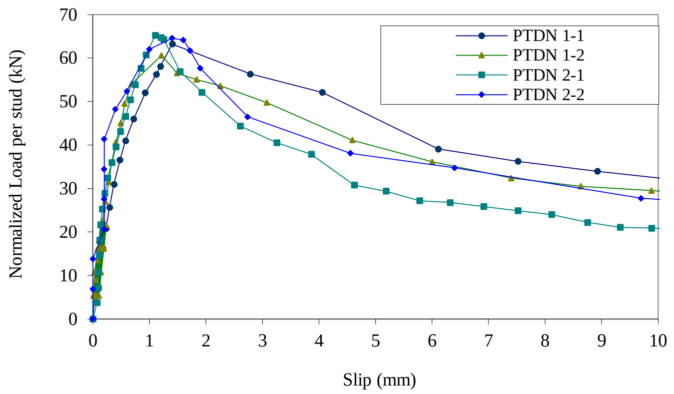


Fig. 16 Effect of shear stud arrangement: PTDN 1-studs in all five ribs and PTDN 2 - studs in first four ribs with last rib unstudded.

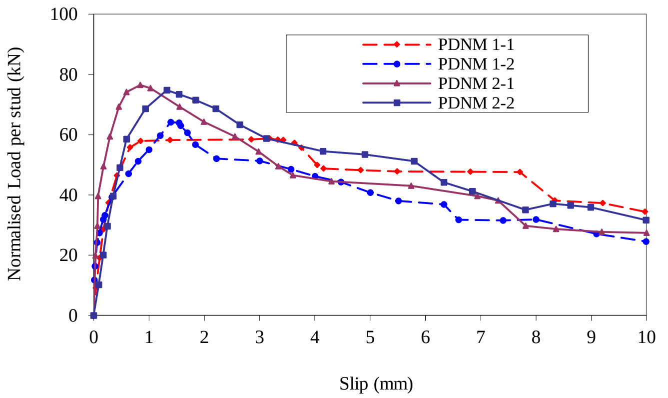


Fig. 17 Effect of shear stud arrangement: PDNM 1-studs in first four ribs (last rib unstudded) and PDNM 2 -studs in middle three ribs (first & last rib unstudded)

### *4.1 Eurocode 4 provisions*

The results are compared with Eurocode 4 (BS EN 1994-1-1 2004) in Table 3. The experimental and theoretical shear connector resistance and slip capacity are worked out as per Eurocode 4 (BS EN 1994-1-1 2004) provisions. The experimental characteristic shear connector resistance, $P_{Rk,e}$ is taken as the failure load per stud in the push test, reduced by 10%. However, this can only be used for tests for which the deviation of any individual test result from the mean test result is less than 10%. In this study, individual test results are within 10% of the mean results of two identical specimens. The slip capacity, $\delta_u$ is taken as the slip at a point where the horizontal line drawn at the characteristic load level touches the falling branch of the load-slip curve. The characteristic slip capacity, $\delta_{uk}$ is taken as the minimum value of the slip capacity, $\delta_u$ reduced by 10%.

$$E_{cm} = 22\left[\frac{f_{cm}}{10}\right]^{0.3} \qquad (f_{cm} \text{ in MPa}) \qquad (2)$$

$$P_{Rk} = k_t \times \left[0.8 f_u \frac{\pi}{4} d^2\right] \qquad (3)$$

$$P_{Rk} = k_t \times \left(0.29 \alpha d^2 \sqrt{f_{ck} E_{cm}}\right) \qquad (4)$$

$$\text{where} \quad k_t = \frac{0.7}{\sqrt{n_r}} \frac{b_0}{h_p}\left(\frac{h_{sc}}{h_p} - 1\right) < k_{t,\max} \qquad (5)$$

$$\alpha = 0.2\left(\frac{h_{sc}}{d} + 1\right) \quad \text{for} \quad 3 \le \frac{h_{sc}}{d} \le 4 \qquad (6)$$

$$\alpha = 1 \quad \text{for} \quad \frac{h_{sc}}{d} > 4 \qquad (7)$$

Table 3 Comparison of experimental and different shear stud strength prediction methods

| Test Ref. | $f_{cm}$ (MPa) | $E_{cm}$ [1] (GPa) | $P_e$ (kN) | $\delta$ (mm) | $P_{Rk,e}$ [2] (kN) | $P_{Rk,t}$ [3] (kN) | $\delta_u$ (mm) | $\delta_{uk}$ [2] (mm) | $P_{Rk,e}$ / $P_{Rk,t}$ | $P_{r\text{-}J\&Y}$ (kN) | $P_{Rk,e}$ / $P_{r\text{-}J\&Y}$ | $Q_{n\text{-}AISC}$ (kN) | $P_{Rk,e}$ / $Q_{n\text{-}AISC}$ | $P_{Rm\text{-}Nell}$ (kN) | $P_e$ / $P_{Rm\text{-}Nell}$ |
|---|---|---|---|---|---|---|---|---|---|---|---|---|---|---|---|
| (1) | (2) | (3) | (4) | (5) | (6) | (7) | (8) | (9) | (10) | (11) | (12) | (13) | (14) | (15) | (17) |
| PTS 1-1 | 25.5 | 29.1 | 75.7 | 0.60 | 68.1 | 63.5 | 0.82 | 0.74 | 1.07 | 69.7 | 0.98 | 86.2 | 0.79 | 103.1 | 0.73 |
| PTS 1-2 | 25.5 | 29.1 | 78.8 | 0.70 | 70.9 | 63.5 | 1.38 | 1.24 | 1.12 | 69.7 | 1.02 | 86.2 | 0.82 | 103.1 | 0.76 |
| PTS 2-1 | 20.6 | 27.3 | 69.0 | 1.67 | 62.1 | 52.3 | 3.80 | 3.42 | 1.19 | 59.6 | 1.04 | 67.5 | 0.92 | 94.6 | 0.73 |
| PTS 2-2[4] | 20.6 | 27.3 | 73.8 | 1.41 | 66.4 | 52.3 | 2.18 | 1.96 | 1.27 | 59.6 | 1.11 | 67.5 | 0.98 | 94.6 | 0.78 |
| PTD 1-1[4] | 20.9 | 27.3 | 52.1 | 1.02 | 46.9 | 43.6 | 1.50 | 1.35 | 1.08 | 50.0 | 0.94 | 68.6 | 0.68 | 59.8 | 0.87 |
| PTD 1-2 | 20.9 | 27.3 | 45.4 | 0.94 | 40.9 | 43.6 | 1.60 | 1.44 | 0.94 | 50.0 | 0.82 | 68.6 | 0.60 | 59.8 | 0.76 |
| PTD 2-1 | 21.1 | 27.3 | 52.2 | 1.23 | 47.0 | 43.9 | 1.80 | 1.62 | 1.07 | 50.2 | 0.94 | 69.1 | 0.68 | 60.1 | 0.87 |
| PTD 2-2 | 21.1 | 27.3 | 47.3 | 0.95 | 42.6 | 43.9 | 2.60 | 2.34 | 0.97 | 50.2 | 0.85 | 69.1 | 0.62 | 60.1 | 0.79 |
| PTSN 1-1 | 19.0 | 26.7 | 97.8 | 2.52 | 88.0 | 48.2 | 3.10 | 2.79 | 1.82 | 55.6 | 1.58 | 60.9 | 1.44 | 100.0 | 0.98 |
| PTSN 1-2 | 19.0 | 26.7 | 98.9 | 2.45 | 89.0 | 48.2 | 3.10 | 2.79 | 1.85 | 55.6 | 1.60 | 60.9 | 1.46 | 100.0 | 0.99 |
| PTSN 2-1 | 15.9 | 25.3 | 90.0 | 1.40 | 81.0 | 39.7 | 2.35 | 2.12 | 2.04 | 46.6 | 1.74 | 47.5 | 1.71 | 91.3 | 0.99 |
| PTSN 2-2 | 17.4 | 26.0 | 81.7 | 1.60 | 73.5 | 44.1 | 2.15 | 1.94 | 1.67 | 51.3 | 1.43 | 54.2 | 1.36 | 92.6 | 0.88 |
| PTDN 1-1 | 21.1 | 27.5 | 61.3 | 1.40 | 55.2 | 44.1 | 2.60 | 2.34 | 1.25 | 50.3 | 1.10 | 69.6 | 0.79 | 63.8 | 0.96 |
| PTDN 1-2 | 27.7 | 29.9 | 67.3 | 1.22 | 60.6 | 56.3 | 2.00 | 1.80 | 1.08 | 57.9 | 1.05 | 81.3 | 0.75 | 72.1 | 0.93 |
| PTDN 2-1 | 44.1 | 34.3 | 91.3 | 2.21 | 82.2 | 71.4 | 1.45 | 1.30 | 1.15 | 62.7 | 1.31 | 81.3 | 1.01 | 91.2 | 1.00 |
| PTDN 2-2 | 47.4 | 35.1 | 93.7 | 1.40 | 84.3 | 71.4 | 1.90 | 1.71 | 1.18 | 62.7 | 1.34 | 81.3 | 1.04 | 94.5 | 0.99 |
| PSNM 1-1 | 24.6 | 28.8 | 113.0 | 2.70 | 101.7 | 61.6 | 3.10 | 2.80 | 1.65 | 68.0 | 1.49 | 82.9 | 1.23 | 103.1 | 1.10 |
| PSNM 1-2 | 27.1 | 29.7 | 138.4 | 2.40 | 124.6 | 66.9 | 3.00 | 3.70 | 1.86 | 72.6 | 1.72 | 92.0 | 1.35 | 103.1 | 1.34 |
| PSNM 2-1 | 24.2 | 28.7 | 127.2 | 2.30 | 114.5 | 60.7 | 2.70 | 2.40 | 1.89 | 67.3 | 1.70 | 81.5 | 1.41 | 103.1 | 1.23 |
| PSNM 2-2 | 24.5 | 28.8 | 134.6 | 1.40 | 121.1 | 61.4 | 1.60 | 1.40 | 1.97 | 67.9 | 1.78 | 82.6 | 1.47 | 103.1 | 1.31 |
| PDNM 1-1 | 34.5 | 31.9 | 72.7 | 3.20 | 65.4 | 67.4 | 3.90 | 3.50 | 0.97 | 61.8 | 1.06 | 81.3 | 0.80 | 79.6 | 0.91 |
| PDNM 1-2 | 36.6 | 32.5 | 81.8 | 1.40 | 73.6 | 70.6 | 1.80 | 1.60 | 1.04 | 62.5 | 1.18 | 81.3 | 0.90 | 81.9 | 1.00 |
| PDNM 2-1 | 23.0 | 28.3 | 77.3 | 0.84 | 69.6 | 47.7 | 1.60 | 1.40 | 1.46 | 52.8 | 1.32 | 76.9 | 0.90 | 65.5 | 1.18 |
| PDNM 2-2 | 23.7 | 28.5 | 76.8 | 1.30 | 69.1 | 49.0 | 2.00 | 1.80 | 1.41 | 53.6 | 1.29 | 79.5 | 0.87 | 66.4 | 1.16 |
| | | | | | | | | Mean | 1.38 | | 1.27 | | 1.02 | | 0.97 |
| | | | | | | | | Standard Deviation (SD) | 0.37 | | 0.30 | | 0.32 | | 0.18 |
| | | | | | | | | Coefficient of Variation (COV) | 26.7% | | 24% | | 31.3% | | 18.3% |

Note: computed [1] using Eurocode 2 (BS EN 1992-1-1 2004), [2] using Eurocode 4 Annex B (BS EN 1994-1-1 2004), [3] using Eurocode 4, clause 6.6.3.1 (BS EN 1994-1-1 2004), [4] from Qureshi *et al.* (Qureshi *et al.* 2011)

Compressive cube strength of concrete was converted to compressive cylinder strength using $f_{cm} = 0.75\ f_{cm,cube}$ for 100-mm cubes as suggested by Stark and Van Hove (1991). The reason for using this relation (Stark and Van Hove 1991) rather than the measured cylinder strength is that it gave inconsistent results in some cases due to improper capping of the loading surface in the test machine. The modulus of elasticity of concrete, $E_{cm}$, for push test specimen was calculated using BS EN 1992-1-1 (BS EN 1992-1-1 2004) provisions as given in Eq. (2). The theoretical characteristic resistance, $P_{Rk,t}$ in Table 3, was calculated using Eurocode 4 (BS EN 1994-1-1 2004) provisions using smaller of Eqs. (3) and (4) based on stud shearing or concrete related failure.

For the push test PTS 1 having a single shear stud per rib with low mesh, the average ratio of $P_{Rk,e}$ / $P_{Rk,t}$ is 1.1, which suggests that the results predicted by Eurocode 4 (BS EN 1994-1-1 2004) are conservative; and the average characteristic slip capacity is 0.99 mm. While, in case of the push test PTS 2 having a single stud with top mesh, the average ratio of $P_{Rk,e}$ / $P_{Rk,t}$ is 1.23, and the average characteristic slip capacity is 2.69 mm. Results obtained from Eurocode 4 (BS EN 1994-1-1 2004) for the push test PTS 2 are more conservative than that for PTS 1. Lower slip capacity in PTS 1 than PTS 2 is due to LVDTs being placed at the back of the slab in PTS 1 and on the sides of the slab in PTS 2. The strength predictions using Eurocode 4 (BS EN 1994-1-1 2004) are close to the experimental results for push tests with double studs, PTD 1 and PTD 2. The average ratio of $P_{Rk,e}$ / $P_{Rk,t}$ is 1.01 and 1.02, the average characteristic slip capacity is 1.40 mm and 1.98 mm for push tests PTD 1 and PTD 2, respectively.

The average ratio of $P_{Rk,e}$ / $P_{Rk,t}$ is 1.85 for single stud push tests with normal load, PTSN 1 and PTSN 2, with characteristic slip capacity of 2.8 mm and 2.03 mm. Eurocode 4 (BS EN 1994-1-1 2004) predicted stud resistance highly underestimated the capacity in tests with single stud and normal load. For push tests PTDN 1 and PTDN 2 having double studs per trough with normal load, the average ratio of $P_{Rk,e}$ / $P_{Rk,t}$ is 1.17 with the average characteristic slip capacity of 2.07 mm and 1.5 mm, respectively. The Eurocode 4 (BS EN 1994-1-1 2004) estimations were better in tests with double studs than single stud per rib.

For push tests with a single stud and double mesh layer, PSNM 1 and PSNM 2, the average ratio of $P_{Rk,e}$ / $P_{Rk,t}$ is 1.76 and 1.93, respectively. The average slip capacity for push tests PSNM 1 and PSNM 2 was computed as 3.25 mm and 1.9 mm, respectively. For companion tests with double studs, PDNM 1 and PDNM 2, the average ratio $P_{Rk,e}$ / $P_{Rk,t}$ is 1.0 and 1.4 with slips of 2.6 mm and 1.4 mm. Due to immediate pull-out of shear studs from the first rib in the push test PDNM 1, the strength enhancement due to double mesh layer could not be achieved and this was the reason that the shear connector resistance obtained from it matched well with the Eurocode 4 (BS EN 1994-1-1 2004) predictions. However, the stud strength predictions from Eurocode 4 (BS EN 1994-1-1 2004) for the push test PDNM 2, which had no studs in the first and last rib, were conservative with estimated load per stud being almost 70% of the actual shear connector resistance observed in the experiment.

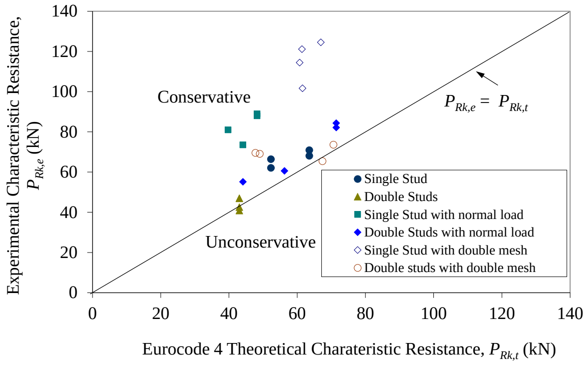


Fig. 18 Experimental versus Eurocode 4 (BS EN 1994-1-1 2004) predicted characteristic resistance

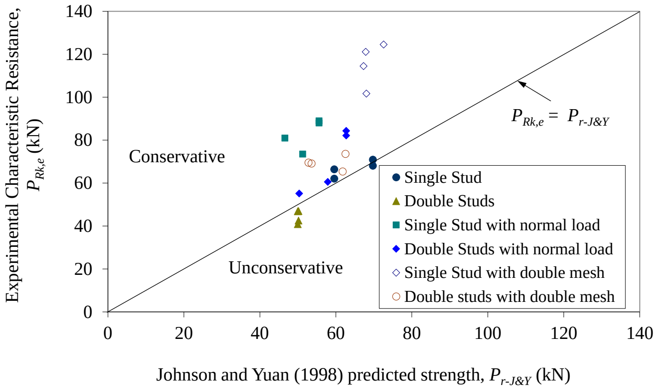


Fig. 19 Experimental versus Johnson and Yuan (Johnson and Yuan 1998) predicted characteristic resistances

Generally, the Eurocode 4 (BS EN 1994-1-1 2004) predictions for push tests having a single stud per rib, double layers of wire mesh and normal load were highly conservative with estimated values nearly equivalent to half of the experimental results.

The predicted characteristic shear connector strengths using Eurocode 4 (BS EN 1994-1-1 2004) equations are compared with experimental characteristic resistances in Fig. 18 and Table 3. It can be seen that Eurocode 4 (BS EN 1994-1-1 2004) estimations are generally conservative for all push tests, except double stud tests without normal load for which the results nearly match the experimental strengths. The average ratio of $P_{Rk,e} / P_{Rk,t}$ is 1.38 with the minimum value of 0.94 and the maximum value of 2.04, and the standard deviation is 0.37 with corresponding coefficient of variation as 26.7%. Conservative estimate of the stud strength provides safety to the structural system but may not be an economical design solution. Design stud resistance is further reduced by dividing the characteristic strength by partial safety factors, normally 1.25 in the UK. As Eurocode 4 (BS EN 1994-1-1 2004) equations are mainly based on push tests without transverse (normal) load, the predicted strength for push tests with normal loads are highly under-estimated, in some cases by as much as 50%.

### 4.2 Johnson and Yuan method

Johnson and Yuan (1998) developed theoretical models for predicting the shear connector resistance depending on the failure modes usually observed in the push test with transverse sheeting. The authors presented theoretical models for five failure modes, namely shank shearing (SS), rib punching (RP), rib punching with shank shearing (RPSS), rib punching with concrete pull-out (RPCP), and concrete pull-out (CPT). However, due to concrete cone failure being the predominant failure mode in this study, only theoretical model for concrete pull-out failure (CPT) is presented here.

The strength of the shear stud according to this method is determined from the following equations

$$P_r = k_{cp} P_{rs} \tag{8}$$

$$P_{rs} = \min \begin{pmatrix} 0.29 d^2 \sqrt{f_{ck} E_{cm}} \\ 0.8 \dfrac{\pi}{4} d^2 f_u \end{pmatrix} \tag{9}$$

$$k_{cp} = \frac{\eta_{cp} + \lambda_{cp}\left(1 - \eta_{cp}{}^2 + \lambda_{cp}{}^2\right)^{0.5}}{1 + \lambda_{cp}{}^2} \leq 1.0 \tag{10}$$

$$\eta_{cp} = \frac{0.56 v_{tu} h^2 \left( b_o - \frac{h}{4} \right)}{h_p N_r P_{rs}} \leq 1.0 \tag{11}$$

$$\lambda_{cp} = \frac{e_r T_y}{h_p P_{rs}} \tag{12}$$

$$T_y \cong 0.8 A_s f_u \tag{13}$$

$$v_{tu} = 0.8 f_{cu}^{\;0.5} \leq 5 \tag{14}$$

The Johnson and Yuan (Johnson and Yuan 1998) predicted shear connector strengths are compared with experimental shear connector resistances in Table 3 and Fig. 19. The shear connector resistance predicted by Johnson and Yuan (1998) method is denoted by $P_{r\text{-}J\&Y}$ in Table 3. The mean ratio of the experimental over Johnson and Yuan (1998) predicted characteristic resistance is 1.27; the standard deviation is 0.30 and the coefficient of variation is 24%. The minimum and maximum values of the average ratio of experimental over predicted strength are 0.82 and 1.78, respectively. Generally, Johnson and Yuan (1998) method gave good estimation of the shear connector resistance, especially for push tests without normal load. The strength predictions for push tests with normal load were highly conservative because the theoretical model on which Johnson and Yuan equations (Johnson and Yuan 1998) are based, does not have any consideration for normal load.

### 4.3 AISC 360-16 provisions

The shear connector resistances obtained from push tests are compared with the strengths of shear stud calculated using AISC 360-16 (ANSI/AISC 360-16 2016) provisions. This code considers different positions of shear stud, namely favourable, central and unfavourable within a sheeting pan and the default value for the shear connector resistance is set equal to the equation for unfavourable position stud. AISC 360-16 (ANSI/AISC 360-16 2016) code makes no distinction between shear stud strength equations for studs placed in a solid concrete or composite slab and uses a common equation for both types of slabs. According to AISC 360-16 (ANSI/AISC 360-16 2016) provisions, the nominal strength of the shear stud embedded in solid concrete or in a composite slab is given by following equation

$$Q_n = 0.5 A_{sc} \sqrt{f_c' E_c} \leq R_g R_p A_{sc} F_u \tag{15}$$

The shear stud strengths obtained from push test experiments are compared with AISC (ANSI/AISC 360-16 2016) predicted strengths in Table 3 and Fig. 20. The shear connector resistance estimated from AISC (ANSI/AISC 360-16 2016) provisions is denoted by $Q_{n\text{-AISC}}$ in Table 3. The average ratio of experimental over AISC (ANSI/AISC 360-16 2016) predicted shear connector strengths is 1.02 with a minimum and maximum value of 0.6 and 1.71, respectively; the standard deviation is 0.32, and the coefficient of variation is 31.2%. Although the mean of the experimental over predicted strength is 1.02, which is close

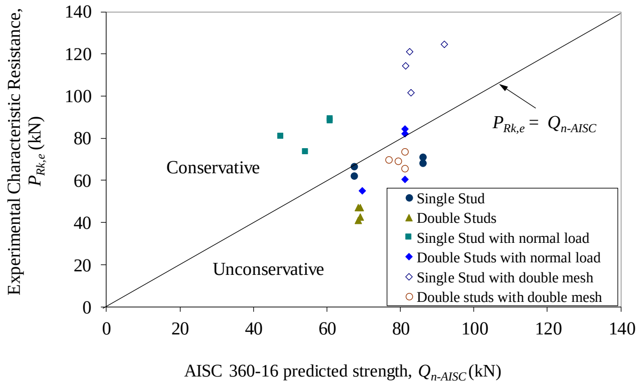


Fig. 20 Experimental versus AISC 360-16 (ANSI/AISC 360-16 2016) predicted characteristic resistances

to 1 as desired. But, the coefficient of variation is significantly large, which indicates high scatter in the data. Apart from single stud push tests with normal load, the AISC (ANSI/AISC 360-16 2016) predicted strengths generally over-estimated connector capacity as shown in Fig. 20.

It is interesting to note that the stud resistance from AISC (ANSI/AISC 360-16 2016) equations gives same strength for tests with single or double studs per rib, when $f_{cm}$ is less than 24 N/mm$^2$ ($f'_c$ or $f_{ck}$ =16 N/mm$^2$) because left side of the Equation 15 dominates in that case. Results show that the strength of the stud placed in pairs is about 70% of the strength from test with a single stud per trough, when no normal is used. Further, it is widely accepted that the load per stud obtained from push tests with pairs of shear connectors per rib is always less than the single stud.

### 4.4 Nellinger equations

Based on push test results with normal load, Nellinger *et al.* (2018) developed new equations for shear connector resistance using a mechanical model. The steel failure in stud is predicted by a plastic stress distribution in the stud using Eq. (16). The resistance of concrete failure is equal to the elastic resistance of the concrete rib in bending and compression in addition to the plastic bending resistance of the shear stud. It is estimated by Eq. (17). The mean shear connector resistance is the smaller of the stud and concrete rib resistance in Eqs. (16) and (17), respectively.

$$P_{\mathrm{Rm}} = 1.26 \left(\frac{f_{\mathrm{uk}}}{\sqrt{3}}\right) \pi d^2/4 \tag{16}$$

$$P_{\mathrm{Rm}} = 1.23\left[\frac{[\alpha_{\mathrm{ct}} f_{\mathrm{ctm}} + (N_{\mathrm{q}} + N_{\mathrm{sc}})/A]W + N_{\mathrm{sc}} e_1}{h_{\mathrm{p}}\; n_r} + \frac{n_y M_{\mathrm{PL}}}{h_{\mathrm{s}} - d/2}\right] \tag{17}$$

$$N_{\mathrm{sc}} = 0.1\, n_{\mathrm{r}} f_{\mathrm{uk}}\; \pi d^2/4 \tag{18}$$

$$A = [2.4 h_{\mathrm{sc}} + (n_{\mathrm{r}} - 1)\, e_{\mathrm{s}}]\, b_{\max} \tag{19}$$

$$W = \frac{1}{6}\ [2.4h_{sc} + (n_r - 1)\ e_s]\ \frac{b_{max}^3}{b_o} \quad (20)$$

$$n_y = 2 \text{ for } h_{sc} \geq h_p + 2d\ \sqrt{n_r} \quad (21)$$

$$n_y = 1 \text{ for } h_{sc} < h_p + 2d\ \sqrt{n_r} \quad (22)$$

$$M_{pl} = f_{uk}\ d^3/6 \quad (23)$$

$$h_s = \frac{\beta h_{sc} + [(n_r - 1)(h_p + h_{sc})e_s]/4.8h_{sc}}{1 + [(n_r - 1)e_s/2.4h_{sc}]} \quad (24)$$

Where $\alpha_{ct}$ = 0.85, $\beta$ = 0.45 for trapezoidal decking, and $\beta$ = 0.41 for re-entrant decking.

The predicted strengths by Nellinger *et al.* (2018) and experimental stud resistance are compared in Table 3 and Fig. 21, where $P_{Rm\text{-}Nell}$ represents the predicted mean shear resistance of headed studs obtained from lesser of Eqs. (16) and (17). These equations are developed and calibrated based on experimental load per stud in push tests with normal load, rather than nominal or characteristic value of load. This is the reason for using the experimental stud resistance, instead of its characteristic value, in all comparisons in Fig. 21. Nellinger *et al.* (2018) themselves used experimental shear stud resistance when comparing their predicted strengths. In Table 3, the ratio of experimental over and Nellinger *et al.* (2018) predicted strengths is 0.97 with standard deviation of 0.18 and coefficient of variation of 18.3%. This method gave the closest prediction with stud resistances over-estimated by only 3% on average. This finding is not different to what was observed by Nellinger *et al.* (2018), where mean stud resistance was over-predicted by 3% with coefficient of variation of 21%.

Nellinger *et al.* (2018) equations were based on push tests with normal load and therefore the predictions were so close to the push tests with transverse load in this study. Except for push tests with single stud and double mesh (PSNM tests), the predicted results showed a close agreement ($P_e$ / $P_{Rm\text{-}Nell}$ = 1.0, SD=0.09 and CoV=8.8%) with all other normal load push tests. For PSNM tests, Eq. (16) is less than Eq. (17), which means stud failure controls rather than concrete rib failure.

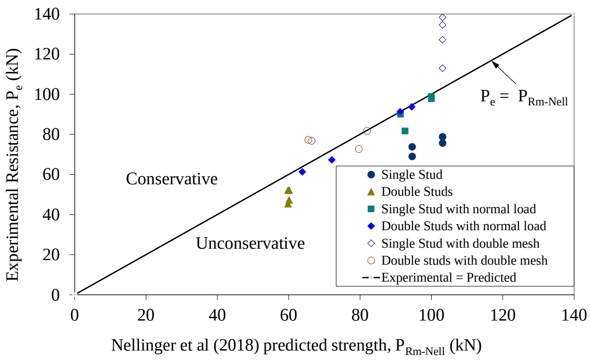


Fig. 21 Experimental versus Nellinger *et al.* (2018) predicted resistances

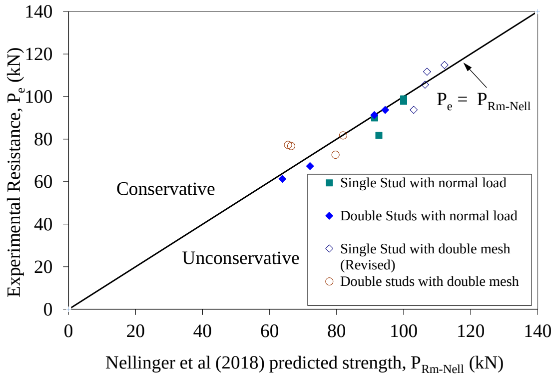


Fig. 22 Revised experimental versus Nellinger *et al.* (2018) predicted resistances for push tests with normal load only

However, concrete related failure was observed in all PSNM tests. In our study, double mesh increased the strength of PSNM tests by 17% compared with single mesh tests (as it is evident in section 3.1).

The correlation between experimental and predicted strengths by Nellinger *et al.* (2018) can be improved further by reducing PSNM results by 17% to account for double mesh effect and by assuming concrete failure in Eq. (17) controls. With revised PSNM results and use of Eq. (17), the predicted mean shear connector resistance compares well with experimental results using normal load ($P_e$ / $P_{Rm\text{-}Nell}$ = 0.99, SD=0.08 and CoV=8.3%). The revised experimental versus predicted shear connector strengths by Nellinger *et al.* (2018) are presented in Fig. 22, which clearly shows an excellent correlation between experimental and predicted load per stud. However, for push test without normal load, Nellinger *et al.* (2018) method over-predicted the strengths by about 20%.

## 5. Conclusions

The results are presented from 24 push test specimens with transverse deck using a horizontal push test setup. Comparison is also made against various shear connector strength prediction methods. Failure modes, shear connector resistance and ductility are discussed. Four main parameters are investigated. First is the effect of wire mesh position - three positions, low (laid directly on top of the steel deck), high (30 mm below the top surface of the concrete slab) and double (combining both low and high positions) are studied. Second is the influence of using a T16 bar at the bottom flange of the steel deck. Third is the effect of normal load and its position relative to the beam axis. Fourth is shear connector arrangement within sheeting ribs – three configurations are tried with studs in all five ribs, first four ribs and middle three ribs. Finally, the experimental results are compared with strength prediction methods from Eurocode 4 (BS EN 1994-1-1 2004) equations, Johnson and Yuan (Johnson and Yuan 1998) method, AISC 360-16 (ANSI/AISC 360-16 2016) provisions and Nellinger *et al.*

(2018) equations. Following are the main findings from this study:

- Locating mesh on top of the steel deck flange or 30 mm from top of the concrete slab does not give any additional benefit in terms of strength and ductility of the headed stud. Eurocode 4 (BS EN 1994-1-1 2004) requires the mesh to be placed 30 mm below the stud's head, indirectly referring to using mesh on top of the steel deck. Current practice in composite industry is to locate the mesh at a nominal cover from top of the concrete slab for controlling temperature and shrinkage cracking. With no extra advantage of using low or high mesh, it can be located anywhere within the steel decking. However, using a double mesh layer resulted in 17% increase in stud strength for push tests with single stud per rib and no increase for tests with double studs/rib.
- Suspending a bar at bottom of the decking trough neither affects strength nor ductility of the headed stud. This is due to concrete failure surfaces not crossing the bar. Using a spiral reinforcement around stud or a waveform reinforcement pattern, as in Ernst *et al.* (2009, 2010) and Patrick (2000), could have increased the stud strength. This is contrary to the recommendations by Kingspan (2011) suggesting a 16 mm diameter reinforcement bar in every trough of their multideck 146 mm deep profiled sheeting for composite action and fire design performance. Thus, using a reinforcement bar at the bottom of the trough is redundant and does not contribute to composite beam action. It might improve the flexural behaviour of composite slab with deep decking though.
- Using a normal load of 10% of the shear load resulted in 40% and 23% increase in the shear stud strength for tests with single and double studs per rib. The strength enhancement in a single stud/rib was twice as much as the double studs per rib. The stud strength depends on how large concrete failure cones are around the stud. In double studs, the failure cones are shared between two studs and cannot develop fully. The position of normal load, either parallel or perpendicular to the beam axis, did not have any influence on strength and ductility of the stud.
- Having no stud in last rib prevented unwanted back-breaking failure and last rib did not rotate at all. However, keeping last rib unstudded did not have any effect on load carrying or slip capacity of the stud. Using studs only in the middle three ribs resulted in 23% increase in the stud strength in comparison to the layout with last rib unstudded.

The shear connector resistance obtained from experimental push tests was compared with the existing strength prediction methods. Eurocode 4 (BS EN 1994-1-1 2004) equations and Johnson and Yuan (1998) method gave good predictions, within 10% of the characteristic experimental load, for first series without normal load and these predictions were generally conservative. Eurocode 4 (BS EN 1994-1-1 2004) highly under-estimated the stud capacity for tests with normal load, in some cases by as much as 50%.

Johnson and Yuan (1998) also under-predicted the shear strength by about 42% for tests with transverse load. AISC 360-16 (ANSI/AISC 360-16 2016) predicted strengths were mostly unconservative, except for tests with single studs and normal load. Nellinger *et al.* (2018) equations precisely estimated the shear stud resistance for tests with normal load with ratio of experimental versus predicted strengths as 0.99 with coefficient of variation of about 8%. However, Nellinger *et al.* (2018) method over-predicted the stud strength in tests without normal load by about 20%.

## Acknowledgments

The authors would like to acknowledge Universities of Leeds, Bradford and East London, and MCRMA for supporting the project.

## References

ANSI/AISC 360-16. (2016), Specification for Structural Steel Buildings. American Institute of Steel Construction (AISC), Chicago, Illinois, USA.

Bonilla, J., Bezerra, L.M., Mirambell, E. and Massicotte, B. (2018), "Review of stud shear resistance prediction in steel-concrete composite beams", *Steel Compos. Struct.*, **27**(3), 355–370. https://doi.org/10.12989/scs.2018.27.3.355.

Bradford, M.A., Filonov, A. and Hogan, T.J. (2006), "Push testing procedure for composite beams with deep trapezoidal slabs", *Proceedings of the 11th, International Conference On Metal Structures*; Progress In Steel, Composite And Aluminium Structures (ICMS-2006), Rzeszow, Poland.

BS EN 1992-1-1. (2004), Eurocode 2: Design of concrete structures, Part 1-1: General rules and rules for buildings, British Standards Institution, London, UK.

BS EN 1994-1-1. (2004), Eurocode 4: Design of composite steel and concrete structures, Part 1-1: General rules and rules for buildings, British Standards Institution, London, UK.

BS EN ISO 6892-1. (2009), Metallic materials — Tensile testing. Part 1: Method of test at ambient temperature, British Standards Institution, London, UK.

David Collings. (2013), Steel–concrete Composite Bridges: Designing with Eurocodes. ICE Publishing, London, UK.

Easterling, W.S., Gibbings, D.R. and Murray, T.M. (1993), "Strength of shear studs in steel deck on composite beams and joists", *Eng. J.*, **30**(2), 44-54.

Ernst, S., Bridge, R.Q. and Wheeler, A. (2009), "Push-out tests and a new approach for the design of secondary composite beam shear connections", *J. Constr. Steel Res.*, **65**(1), 44–53. https://doi.org/10.1016/j.jcsr.2008.04.010.

Ernst, S., Bridge, R.Q. and Wheeler, A. (2010), "Correlation of beam tests with pushout tests in steel-concrete composite beams", *J. Struct. Eng.*, **136**(2), 183–192. https://doi.org/10.1061/(ASCE)0733-9445(2010)136:2(183).

Hicks, S. (2007), "Strength and ductility of headed stud connectors welded in modern profiled steel sheeting", *Structural Engineer*, **85**(10), 32–38.

Hicks, S. and Couchman, G. (2004), "The shear resistance and ductility requirements of headed studs used with profiled steel sheeting", *Proceedings of the 5th International Conference on Composite Construction in Steel and Concrete*, Kruger National Park, Berg-en-Dal, Mpumalanga, South Africa, July 18-23.

Hicks, S.J. and Smith, A.L. (2014), "Stud shear connectors in composite beams that support slabs with profiled steel sheeting", Structural Engineering International: Journal of the International Association for Bridge and Structural Engineering (IABSE), **24**(2), 246-253. https://doi.org/10.2749/101686614X13830790993122.

Huo, J., Wang, H., Li, L. and Liu, Y. (2019), "Experimental study on impact behaviour of stud shear connectors in composite beams with profiled steel sheeting", *J. Constr. Steel Res.*, **161**, 436-449. https://doi.org/10.1016/j.jcsr.2018.04.029.

Johnson, R.P. and Yuan, H. (1998), "Models and design rules for stud shear connectors in troughs of profiled sheeting", *Proceedings of the Institution of Civil Engineers - Structures and Buildings*, **128**(3), 252-263. https://doi.org/10.1680/istbu.1998.30459.

Kingspan. (2011), "Multideck Technical Handbook, Manufactures of Multideck Composite Metal Decking." North Yorkshire, United Kingdom, <https://www.kingspan.com/gb/en-gb/products/structural-steel-solutions/structural-steel products/ downloads#!hp=18098&rs_np_1=p-64348&p=1&ps=16> (Sep. 4, 2019).

Lloyd, R.M. and Wright, H.D. (1990), "Shear connection between composite slabs and steel beams", *J. Constr. Steel Res.*, **15**(4), 255-285. https://doi.org/10.1016/0143-974X(90)90050-Q.

Nellinger, S., Eggert, F., Kuhlmann, U., Odenbreit, C. and Obiala, R. (2018), "Short-span composite beam tests to evaluate stud resistances", *Proceedings of the Institution of Civil Engineers: Structures and Buildings*, **171**(1). https://doi.org/10.1680/jstbu.16.00173.

Nellinger, S., Odenbreit, C. and Lawson, R.M. (2014), "Push-out tests with modern deck sheeting and realistic transverse loading", *Proceedings of the 12th International Conference on Steel, Space and Composite Structures*, Prague, Czech Republic, 28-30 May.

Nellinger, S., Odenbreit, C., Obiala, R. and Lawson, M. (2017), "Influence of transverse loading onto push-out tests with deep steel decking", *J. Constr. Steel Res.*, **28**, 335-353. https://doi.org/10.1016/j.jcsr.2016.08.021.

Patrick, M. (2000), "Experimental investigation and design of longitudinal shear reinforcement in composite edge beams", *Progress Struct. Eng. Mater.*, **2**(2), 196-217. https://doi.org/10.1002/1528-2716(200004/06)2:2<196::AID-PSE22>3.0.CO;2-2.

Qureshi, J. (2010), "Finite element modelling of steel-concrete composite structures", PhD Thesis, University of Leeds, Leeds, UK. Retrieved from http://etheses.whiterose.ac.uk/id/eprint/21112.

Qureshi, J., Lam, D. and Ye, J. (2011), "Effect of shear connector spacing and layout on the shear connector capacity in composite beams", *J. Constr. Steel Res.*, **67**(4), 706-719. https://doi.org/10.1016/j.jcsr.2010.11.009.

Rambo-Roddenberry, M.D. (2002), "Behavior and Strength of Welded Stud Shear Connectors", PhD Thesis, Virginia Polytechnic and State University, Blancksburg, Virginia, USA. Retrieved from https://vtechworks.lib.vt.edu/handle/10919/26989.

Shen, M.H. and Chung, K.F. (2017a), "Structural Behaviour of Stud Shear Connections with Solid and Composite Slabs Under Co-Existing Shear and Tension Forces", *Structures*, **9**, 79-90. https://doi.org/10.1016/j.istruc.2016.09.011.

Shen, M.H. and Chung, K.F. (2017b), "Experimental investigation into stud shear connections under combined shear and tension forces", *J. Constr. Steel Res.*, **133**, 434–447. https://doi.org/10.1016/j.jcsr.2017.02.021.

Smith, A.L. and Couchman, G.H. (2010), "Strength and ductility of headed stud shear connectors in profiled steel sheeting", *J. Constr. Steel Res.*, **66**(6), 748–754. https://doi.org/10.1016/j.jcsr.2010.01.005.

Stark, J. and Van Hove, B.W.E.M. (1991)., Statistical analysis of push-out tests on stud connectors in composite steel and concrete structures. TNO Building and Construction Research Report BI-91-163, Delft, The Netherlands.

Sun, Q., Nie, X., Denavit, M.D., Fan, J. and Liu, W. (2019), "Monotonic and cyclic behavior of headed steel stud anchors welded through profiled steel deck", *J. Constr. Steel Res.*, **157**, 121-131. https://doi.org/10.1016/j.jcsr.2019.01.022.

*CC*

## Notations

$A_s$ Cross section area of shear connector stud

$A_{sc}$ cross-sectional area of stud shear connector, mm$^2$

$b_o$ Average width of rib of profiled steel decking

$b_o$ width at top of rib in Nellinger *et al.*

$b_{max}$ Largest width of deck rib

$d$ Diameter of the shank of the stud, 16 mm ≤ $d$ ≥ 25 mm

$e_1$ Eccentricity of stud to centreline of rib

$e_s$ Transverse spacing between studs

$e_{mid\text{-}ht}$ distance from the edge of stud shank to the steel mid-height of deck web, in the load bearing direction of the stud (in other words, in the direction of maximum moment for a simply supported beam), mm

$e_r$ distance from center of stud to nearer wall of rib for favourable position studs

$E_c$ modulus of elasticity of concrete = $0.043 w_c^{1.5}\sqrt{f_c'}$, MPa

$E_{cm}$ Secant modulus of elasticity of concrete (kN/mm$^2$)

$f_c'$ specified minimum compressive strength of concrete, MPa

$f_{ck}$ characteristic cylinder strength of concrete

$f_{cm,cube}$ Mean value of concrete cube compressive strength (N/mm$^2$)

$f_{cu}$ Compressive cube strength of concrete

$f_{cm}$ Mean value of concrete cylinder compressive strength (N/mm$^2$)

$f_{ctm}$ Tensile strength of concrete (N/mm$^2$)

$f_u$ Specified ultimate strength of the stud material but not greater than 450 N/mm$^2$ for composite slab with profiled sheeting.

$f_{uk}$ Characteristic tensile strength of stud material

$F_u$ specified minimum tensile strength of a stud shear connector, MPa

$h$ height of stud

$h_p$ Overall depth of the profiled steel sheeting excluding embossments

$h_{sc}$ Overall nominal height of a stud connector

$k_{cp}$ reduction factor for CPT failure mode

$\eta_{cp}$ non-dimensional group for CPT failure mode

$\lambda_{cp}$ non-dimensional group for CPT failure mode

$k_t$ Reduction factor based on the dimensions of the steel deck and the number of shear connectors per trough when the profiled sheeting is transverse to the beam, only applicable when $h_p$ is not greater than 85 mm and a width $b_0$ not less than $h_p$.

$k_{t,max}$ Maximum value of reduction factor, for single shear stud per trough: $k_t = 0.85$ for sheeting thickness $t \le 1$ mm and $k_t = 1$ for $t > 1$ mm, for double shear studs per trough: $k_t = 0.7$ for $t \le 1$ mm and $k_t = 0.8$ for $t > 1$ mm. These values are valid for through welded shear stud not exceeding 20 mm in diameter.

$N_q$ transverse compressive force per deck rib

$N_r$ number of studs per rib

$n_r$ Number of shear connectors in one rib, not exceeding 2.

$\eta_y$ Number of yield hinges in the stud shank

$P_e$ Experimental maximum load per stud (kN)

$P_{e,\,norm}$ Normalised experimental maximum load per stud (kN)

$P_{Rk}$ Characteristic resistance of a shear connector

$P_{Rk,e}$ Experimental Characteristic Resistance (kN)

$P_{Rk,t}$ Theoretical Characteristic Resistance (kN) using Eurocode 4

$Q_{n\text{-AISC}}$ Nominal unfactored design strength calculated from AISC 360-16

$P_{r\text{-}J\&Y}$ Shear connector resistance per stud obtained from Johnson and Yuan method

$P_{Rm\text{-}NEll}$ Shear connector resistance per stud obtained from Nellinger *et al.* method

$P_{rs}$ shank shearing resistance of the stud in a solid concrete slab

$R_g$ Group effect factor having values equal to 1, 0.85 and 0.7 for one, two and three or more studs welded in a steel deck rib with the deck oriented perpendicular to the steel shape.

$R_p$ Position effect factor

= 1 for studs embedded in solid concrete slab

= 0.75 for studs welded in *composite* slab with the deck oriented perpendicular to the *beam* and $e_{mid\text{-}ht} \ge 50$ mm (favourable position studs)

= 0.6 for studs welded in *composite* slab with the deck oriented perpendicular to the *beam* and $e_{mid\text{-}ht} < 50$ mm (unfavourable position studs)

$T_y$ Resistance of shear stud to uniaxial tension

$v_{tu}$ Shear strength of concrete

$\delta$ Maximum slip at failure (mm)

$\delta_u$ Slip Capacity (mm)

$\delta_{uk}$ Characteristic slip capacity (mm)